Supporting Information

Curtale et al. 10.1073/pnas.1219852110

SI Materials and Methods

Reagents. LPS from *Escherichia coli* (serotype 055:B5), Pam_3CsK_4, imiquimod, synthetic CpG oligonucleotides (ODN) and poly(I:C) were purchased from Enzo Life Sciences. Human IL-10 and IL-1β were purchased from R&D Systems. AG-490 was purchased from Calbiochem. Rabbit anti-Myd88 antibody was purchased from Enzo Life Science, and rabbit anti–IRAK-1 and rabbit anti-TRAF6 antibodies from Cell Signaling Technology. Other antibodies were purchased from Biolegend unless specified otherwise.

Purification of Murine Macrophages. Mouse macrophages, obtained from 6- to 8-wk C57BL/6 mice, were plated in six-well plates at a density of 1 to $2 \times 10^5/cm^2$. Femora and tibiae of hind legs were flushed with PBS solution and cells were resuspended in Iscove's modified Dulbecco's medium (IMDM) medium with L-glutamine, 10% (vol/vol) FCS, 100 U/mL penicillin, and 100 mg/mL of streptomycin and cultured for 7 d with 10 ng/mL macrophage colony-stimulating factor (MCSF). Macrophages were detached using PBS solution containing 10 mM EDTA, washed, and resuspended in IMDM medium supplemented with, 10% heat-inactivated FCS, 100 U/mL of penicillin, and 100 mg/mL of streptomycin.

Lentiviral Constructs. The pCR2.1 vector (Invitrogen) was used as subcloning vector. For THP-1 cells transduction, the microRNA (miR)/lentiviral-based expression vector pRRL-miR-146b and premiR-146a were generated cloning a 500-bp region encompassing the premiR-146b and premiR-146a in the pRRLSIN.cPPT. PGK-GFP.WPRE vector (plasmid 12252; Addgene). The lentiviral construct pRRL-ctrl, encoding for a hairpin yielding a 22-mer RNA with no homology to any human gene, was used as mock construct.

ChIP Assay. Sheared chromatin from 5×10^6 monocytes was immunoprecipitated overnight (ON) at 4 °C by using polyclonal antibodies against polymerase II (N-20; sc-899; Santa Cruz Biotechnology), STAT3 (C-20; sc-482; Santa Cruz Biotechnology). One percent of starting chromatin was used, not immunoprecipitated, and used as input. Quantitative real-time PCR (qPCR) was performed in triplicate by using promoter-specific primers (Table S1). Signals obtained from the ChIP samples were normalized on signals obtained from corresponding input samples, according to the formula $100 \times 2^{\wedge(\text{input Ct} - \text{sample Ct})}$. Results were expressed as fold enrichment relative to untreated cells.

Quantification of miR and mRNA. Total RNA was reverse transcribed and quantification was performed by using Power SYBR Green Mix (Applied Biosystems) with specific primer pairs (Table S1). Experimental data were then analyzed using the SDS2.2 software, and the relative expression values were calculated according to the "comparative Ct" method using U6 as endogenous control for miR and GAPDH for mRNA.

Luciferase Reporter Assay. HEK-293T cells were plated in 24-well plates in 500 μL of D-MEM supplemented with 10% FBS and 1% of L-glutamine at 16×10^4 per well. After 24 h, cells were transfected with 100 ng psiCHECK-2–3′UTR reporter construct and 700 ng pcDNA3-miR or pcDNA3 as control by using Lipofectamine 2000 (Invitrogen). After 48 h, cells were lysed, and *firefly* and *renilla* luciferase activities were determined by using the Dual-Glo Luciferase Assay System (Promega). The enzymatic activities of both luciferases were quantified by using a MultiDetection Microplate Reader Synergy 2 luminometer (BioTek). The values of *renilla* luciferase activity were normalized by *firefly* luciferase activities, which served as internal control. Normalized values were expressed as fold changes relative to the value of the negative control.

***In Silico* Prediction of miR-146b Targets.** The list of miR-146b predicted targets with their probability (mirSVR) score was obtained from the microRNA database (www.microrna.org) (1). The relative enrichment of biological functions and associated networks was determined calculating the *P* value associated to the Fisher exact test built into the Ingenuity Pathway Analysis software (Ingenuity Systems).

Immunoprecipitation of Ago2-Bound RNAs. Immunoprecipitations were carried out ON at 4 °C by using Magna Chip Protein A+G magnetic beads (Millipore) conjugated with anti-Ago2 (EIF2C2 monoclonal antibody, clone 2E12-1C9; Abnova) or isotype IgG_{1k} control Abs (Abnova). A total of 30×10^6 pRRL-ctrl and pRRL-146b THP-1 cells were stimulated for 2 h with 1 μg/mL LPS, whereas miRzip-ctrl and miRzip-146b THP-1 cells were stimulated for 12 h with 1 μg/mL LPS. In all experiments, an aliquot of immunoprecipitation supernatants, corresponding to 0.5×10^6 cell equivalent, was removed after immunoprecipitation (indicated as "left over") and used as control for the specificity of the assay. Results were expressed as fold enrichment relative to Ago2-IP CT samples. Sequences of 3′UTR mRNA-specific primers used in qPCR are listed in Table S1. The miR/mRNA enrichment to the RNA-induced silencing complex was calculated according to the formula $2^{-(\text{CtAgo} - \text{CtIgG})}$ and normalized over GAPDH for mRNA and U6 for miR.

Prediction of miRNA–mRNA Duplex Secondary Structure. The RNAhybrid Web server (http://bibiserv.techfak.uni-bielefeld.de/rnahybrid) (2) was used to predict multiple binding sites of miRNAs in large target RNAs, calculating the minimum free energy related to the secondary structure of the miRNA–mRNA duplex.

1. Hendrickson DG, Hogan DJ, Herschlag D, Ferrell JE, Brown PO (2008) Systematic identification of mRNAs recruited to argonaute 2 by specific microRNAs and corresponding changes in transcript abundance. *PLoS ONE* 3(5):e2126.

2. Rehmsmeier M, Steffen P, Hochsmann M, Giegerich R (2004) Fast and effective prediction of microRNA/target duplexes. *RNA* 10(10):1507–1517.

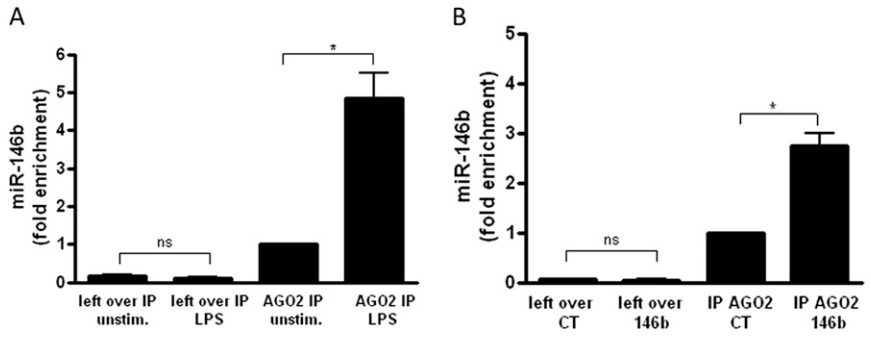

Fig. S1. MiR-146b enrichment in the RISC complex. (*A*) Human monocytes were stimulated or not with 100 ng/mL LPS for 16 h. Cell extracts were subjected to RIP assay using anti-Ago2 or IgG control Abs and levels of miR-146b were assayed in triplicate by Q-PCR in RIP (IP AGO2) and left over samples and expressed as normalized fold enrichment of miR-146b. (*B*) Cell extracts from pRRL-ctrl transduced (CT) and pRRL-146b transduced (146b) THP-1 cells were subjected to RIP assay using anti-Ago2 or IgG control Abs and levels of miR-146b were assayed in triplicate by Q-PCR in RIP (IP AGO2) and left over samples and expressed as normalized fold enrichment of miR-146b. Results are shown as normalized fold enrichment (mean ± SEM).

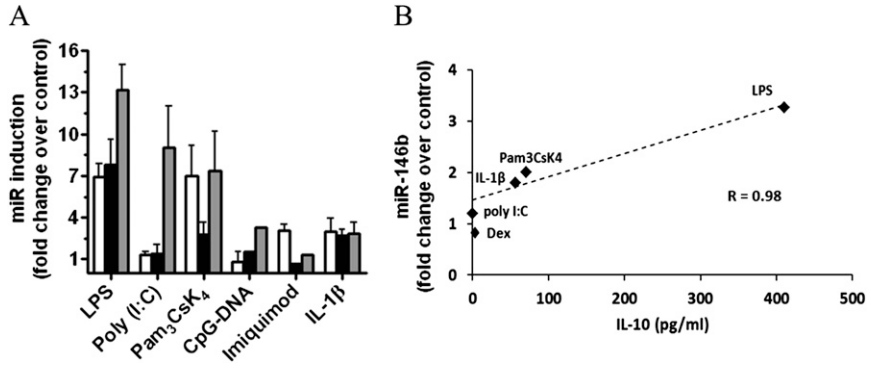

Fig. S2. MiR-146b induction by different stimuli correlates with IL-10 expression. (*A*) Expression levels of miR-146a (white columns), miR-146b (black columns), and miR-155 (grey columns) were measured by Q-PCR in triplicate samples of human monocytes cultured for 24 h with TLR/IL-1R agonists (100 ng/mL LPS, 5 μg/mL poly(I:C), 1 μg/mL Pam_3CsK_4, 1μM CpG-DNA, 100 ng/mL imiquimod, 100 ng/mL IL-1β). Results are expressed as fold change over untreated cells (mean ± SEM; $n = 3$). (*B*) Monocytes were cultured for 24 h with 100 ng/mL LPS, 1 μg/mL Pam_3CsK_4, 5 μg/mL poly(I:C), 100 ng/mL IL-1β, or 200 ng/mL dexamethasone. IL-10 release in cell-free supernatants was analyzed by ELISA and correlated to the expression of miR-146b, quantified by Q-PCR. Dotted line represents the linear regression curve correlating miR-146b expression levels with IL-10 release in the indicated experimental conditions. Results shown are from one representative of three independent experiments.

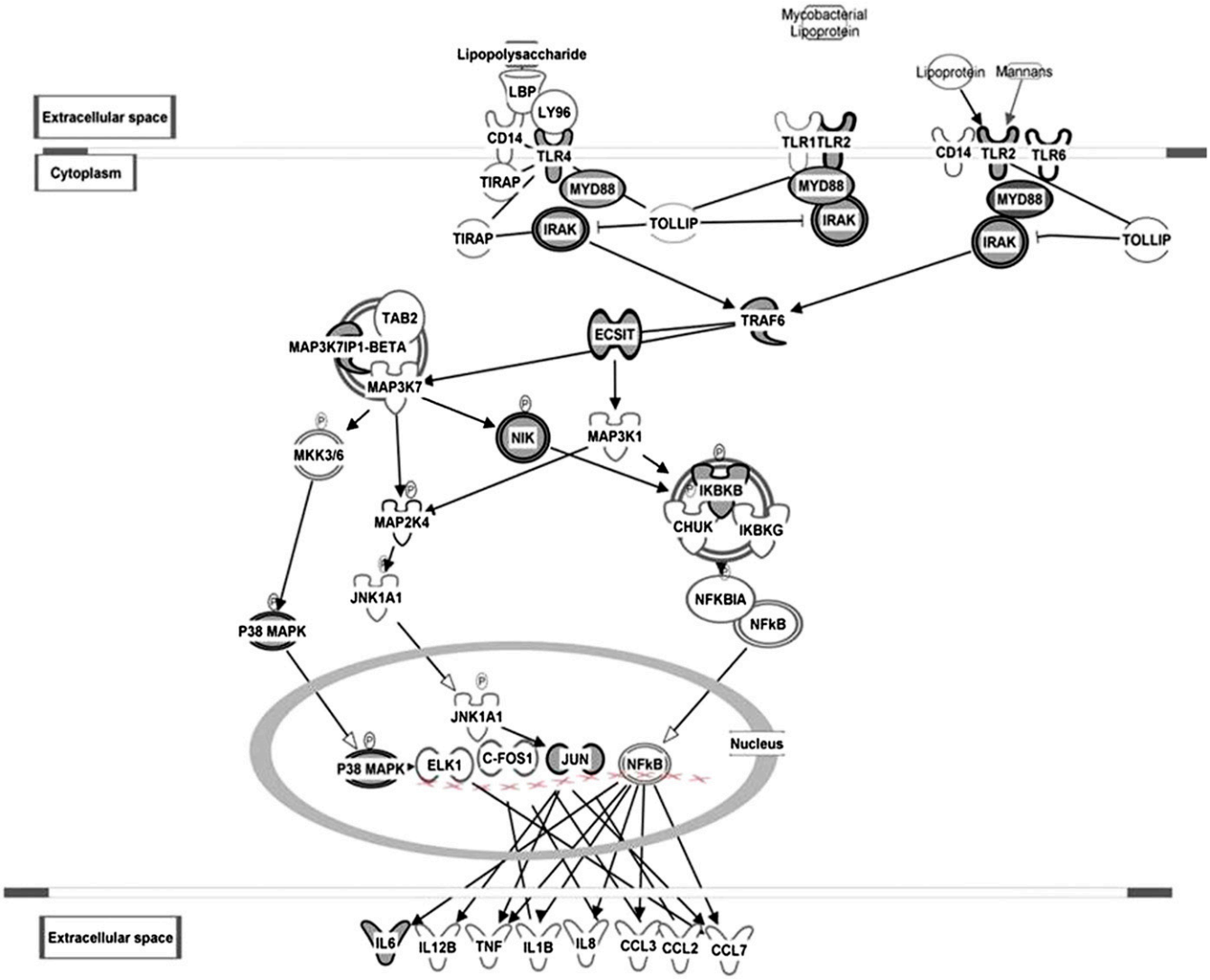

Fig. S3. Predicted miR-146b targets in the TLR pathway. Graphic representation of the TLR4/TRL2 pathway with predicted miR-146b target genes highlighted.

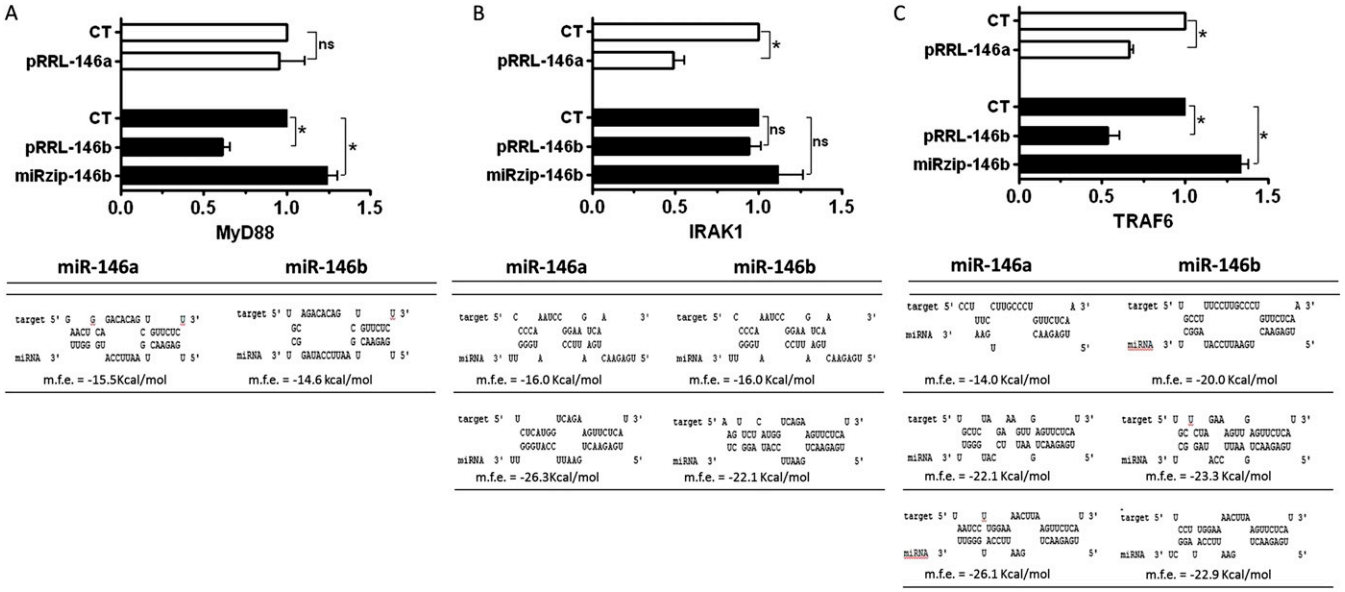

Fig. S4. Differential effect of miR-146a and miR-146b on transcripts of TLR signalling adaptors. Relative MyD88 (*A*), IRAK-1 (*B*), and TRAF6 (*C*) mRNA levels were measured by Q-PCR in pRRL-ctrl, pRRL-146b, miRzip-ctrl and miRzip-146b THP-1 cells and normalized to GAPDH. Results are shown as fold change over nonstimulated control (mean ± SEM). The predicted structure of the miRNA-mRNA target duplex is graphically visualized, according to RNA hybrid algorithm (see *SI Materials and Methods*) and the corresponding minimum free energy (m.f.e.) is also reported.

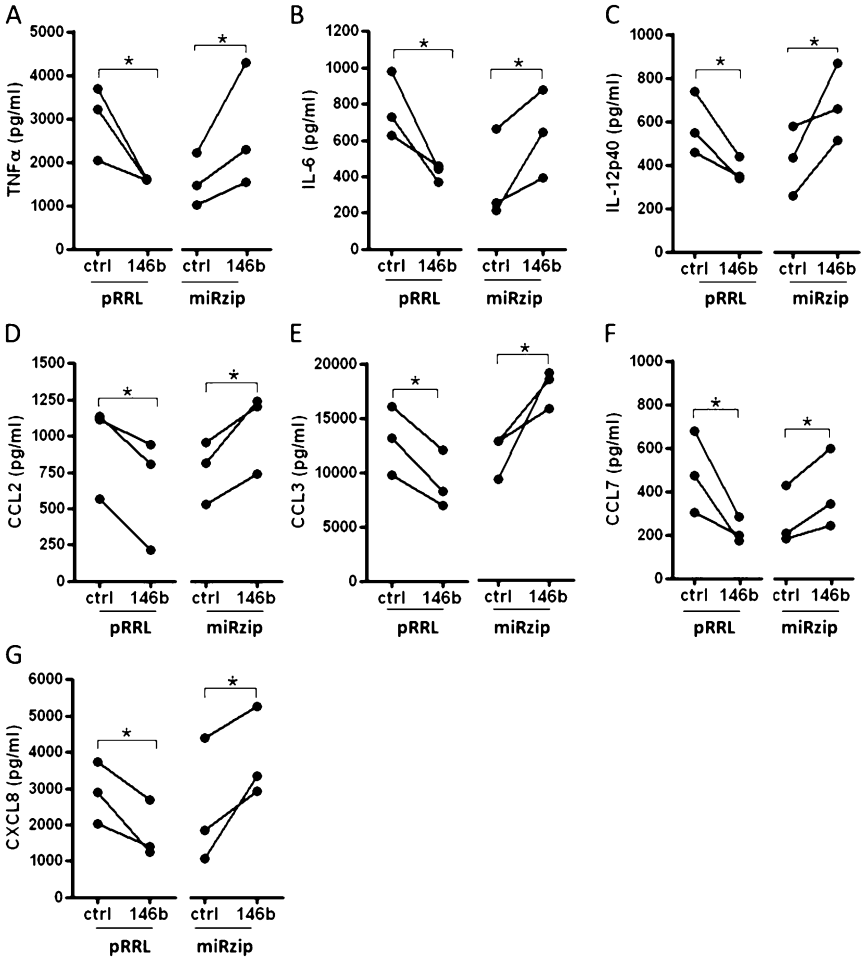

Fig. S5. MiR-146b down-regulates TLR2-dependent production of pro-inflammatory cytokines. (*A–G*) Pro-inflammatory cytokine levels measured by ELISA in cell-free supernatants of THP-1 cells transduced with lentiviral vectors overexpressing miR-146b (pRRL-146b and its respective control) or a miR-146b sponge (miRzip-146b and its respective control) after stimulation with 1 μg/mL Pam_3CsK_4.

Table S1. List of oligonucleotides used

Type	Oligonucleotide
Cloning	
TLR4 3′UTR	5′-GTCAGAAACCTGTCCACT-3′
	5′-TGTGCCTAATTCAGAAGATG-3′
TLR2 3′UTR	5′- GTTCCCATATTTAAGACCAG-3′
	5′- TCTCATCCTGTAAAGTTTAA-3′
IL-6 3′UTR	5′-GTCAGAAACCTGTCCACT-3′
	5′-AATATGTATAAGTTAGCCAT-3′
IRAK-1 3′UTR	5′-ATCATTTATGCTTGGGAGGT-3′
	5′-AAGAGGACACTCGGTTACA-3′
MyD88 3′UTR	5′-GCAAATATCGGCTTTTCTCA-3′
	5′-GACTCTCTTTGGAGCATA-3′
TRAF6 3′UTR	5′-TTGCCCTCACTTGCTCAA-3′
	5′-AGATGCTACTTCGTAACCTC-3′
miR-146b	5′-TGGAATAGGAGTTCTCTTG-3′
	5′-TAGTGGCAGGTTATGAGCA-3′
miR-146b seed mutagenesis	
TLR4	5′-TGTCTATGGCTGTTTGAGATTCTCTACTCTTGTGCTTG-3′
	5′-CAAGCACAAGAGTAGAGAATCTCAAACAGCCATAGACA-3′
IRAK-1 (seed 1)	5′-GATCCCCCAAATCCGGCAAAGTTCTCATGGTC-3′
	5′-GACCATGAGAACTTTGCCGGATTTGGGGGATC-3′
IRAK-1 (seed 2)	5′-GCAAAGTTCTCATGGTCGTTCTCATGGTGCACGA-3′
	5′-TCGTGCACCATGAGAACGACCATGAGAACTTTGC-3′
MyD88	5′-GAACTGCAGACACAGCTTCTCCCTCTCTCCTT-3′
	5′-AAGGAGAGAGGGAGAAGCTGTGTCTGCAGTTC-3′
TRAF6 (seed 1)	5′-CCTGGAGAAAACAGTGTCCTTGCCCTGTTCTC-3′
	5′-GAGAACAGGGCAAGGACACTGTTTTCTCCAGG-3′
TRAF6 (seed 2)	5′-CTCGAGAAGAGTTATTGCTCTAGTTGAGTTCTCATTTTTTTAACC-3′
	5′-GGTTAAAAAAATGAGAACTCAACTAGAGCAATAACTCTTCTC-3′
TRAF6 (seed 3)	5′-ATTTGAACCATAATCCTTGGATTAAGTTCTCATTCACCCCAG-3′
	5′-CTGGGGTGAATGAGAACTTAATCCAAGGATTATGGTTCAAAT-3′
qPCR	
MyD88	5′-GCACATGGGCACATACAGAC-3′
	5′-GACATGGTTAGGCTCCCTCA-3′
IL-6	5′-TACCCCCAGGAGAAGATTCC-3′
	5′-TTTTCTGCCAGTGCCTCTTT-3′
TLR4	5′-CACCTGATGCTTCTTGCTG-3′
	5′-TCCTGGCTTGAGTAGATAA-3′
TRAF6	5′-GTCCCTTCCAAAAATTCCAT-3′
	5′-CACAAGAAACCTGTCTCCTT-3′
IRAK-1	5′-TGAAGAGGCTGAAGGAGAA-3′
	5′-CACAATGTTTGGGTGACGAA-3′
ChIP assay	
Pol-II on miR-146b	5′-AATAGGAGTTCTCTTGGTAT-3′
	5′-AATTCAGTTCTCAGTGCC-3′
Pol-II on miR-146a	5′-GAGGAAGTGACATTGAAAGC-3′
	5′-TGTATGGTAGACACACACAT-3′
Pol-II on miR-155	5′-ACCATTTCTTCCTCTCTTAG-3′
	5′-GGCTCCAACCTTTGTTCTT-3′
STAT3 in miR-146b	5′-CTCGGCTGAACTCTCCAGA-3′
	5′-GCAAACCAAGGGGCTTTCT-3′
STAT3 in miR-146a	5′-GCACTTGAAAAGCCAACAGG-3′
	5′-CACAGCGAGGGAGGAAGA-3′
RIP assay	
IRAK-1	5′-CTCTTTGCCCATCTCTTTG-3′
	5′-GCCACACTTTTCCAAATTGT-3′
TRAF6	5′-TAAGTTCTCATTCACCCCAG-3′
	5′-AGGAAATAAGTAAGCAAGGC-3′
MYD88	5′-GCTTGGGCTGCTTTTCATT-3′
	5′-CCTGCTCACATCATTACAGT-3′
TLR4	5′-CCTCCTCAGAAACAGAACAT-3′
	5′-TCATAACGGCTACACCATTT-3′
TLR2	5′-CAACTGTAATCTGTAGCAAC-3′
	5′-TAGCAGGAAGAAAGAATGAC-3′
IL-6	5′-GCATTCCTTCTTCTGGTCA-3′
	5′-ATAGTGTCCTAACGCTCATA-3′